Heliyon 10 (2024) e29433

Contents lists available at ScienceDirect

Heliyon

journal homepage: www.cell.com/heliyon

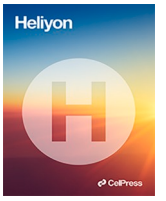

Research article

A sustainable approach to prepare green synthesis of copper nanoparticles of *Bauhinia variegata & Saussurea lappa*: Unveiling *in-vitro* anti-obesity applications

Mukul Kumar [a,*], Deepika Kaushik [b,**], Ashwani Kumar [c], Hari Krishnan [a], Fatih Oz [d], Charalampos Proestos [e], Abeer Hashem [f], Elsayed Fathi Abd_Allah [g]

[a] *Department of Food Technology and Nutrition, Lovely Professional University, Phagwara, 144411, Punjab, India*
[b] *Department of Biotechnology, Faculty of Applied Science and Biotechnology, Shoolini University, Solan, H.P., 173229, India*
[c] *Institution of Food Technology, Bundelkhand University, Jhansi, 284127, India*
[d] *Department of Food Engineering, Faculty of Agriculture, Ataturk University, Erzurum, 25240, Turkiye*
[e] *Laboratory of Food Chemistry, Department of Chemistry, School of Sciences, National and Kapodistrian University of Athens Zografou, 157 84, Athens, Greece*
[f] *Botany and Microbiology Department, College of Science, King Saud University, P.O. Box. 2460, Riyadh, 11451, Saudi Arabia*
[g] *Plant Production Department, College of Food and Agricultural Sciences, King Saud University, P.O. Box. 2460, Riyadh, 11451, Saudi Arabia*

A R T I C L E I N F O

Keywords:
Copper nanoparticles
Bauhinia variegata
Saussurea lappa
Characterization
Lipase inhibition assay
Amylase inhibition assay

A B S T R A C T

Nanoparticles have different shapes and sizes between the range of 1–100 nm, which show advantages for stabilizing compounds, higher carrier capacity, and lower costs. Metal nanoparticles such as copper, gold, silver, and zinc are favorable components for various applications due to their interesting properties. In the present study, nanoparticles were synthesized by reduction with flower extracts of *Bauhinia variegate & Saussurea lappa* that were used to stabilize the copper nanoparticles. Furthermore, the characterization of plants synthesized copper nanoparticles was carried out through UV–visible dynamic light scattering. Additionally, morphological characterization of nanoparticles was confirmed by scanning electron microscopy and energy dispersive X-ray spectroscopy confirmed the elemental composition of copper nanoparticles. Powder X-ray diffraction was conducted for the analysis of crystallinity, purity, and crystal size of plant-synthesized copper nanoparticles. The average particle size was evaluated and exhibited the particle size at the peak of 8.721 nm and 98.03 nm for flower extracts of *Bauhinia variegate & Saussurea lappa* copper nanoparticles. The Fourier Transform Infrared spectrum was taken to scrutinize the various functional groups that were responsible for the reduction of the copper ions. The antimicrobial results against the bacterial strains with the positive test results of the zone of inhibition were for *Bauhinia variegate* (17 mm, 18 mm, 19 mm, and 18 mm) and *Saussurea lappa* (17 mm, 19 mm, 18 mm, and 18 mm) respectively for plants synthesized copper nanoparticles against the *Staphylococcus aureus*, *Escherichia coli*, *Klebsiella pneumonia* and *Pseudomonas aeruginosa.* Lipase inhibition assay and Amylase inhibition assay with different concentrations (20 μg/mL to 100 μg/mL) for *Bauhinia variegate & Saussurea lappa* (12.34 %–59.67 % and 10.50 %–47.01

* Corresponding author.M.K
** Corresponding author.D.K
E-mail addresses: mukulkolish@gmail.com (M. Kumar), dk4275388@gmail.com (D. Kaushik), ashwanichandel480@gmail.com (A. Kumar), harijunior4@gmail.com (H. Krishnan), fatihoz@atauni.edu.tr (F. Oz), harpro@chem.uoa.gr (C. Proestos), habeer@ksu.edu.sa (A. Hashem), eabdallah@ksu.edu.sa (E.F. Abd_Allah).

https://doi.org/10.1016/j.heliyon.2024.e29433
Received 22 February 2024; Received in revised form 8 April 2024; Accepted 8 April 2024
Available online 12 April 2024
2405-8440/© 2024 The Authors. Published by Elsevier Ltd. This is an open access article under the CC BY-NC license (http://creativecommons.org/licenses/by-nc/4.0/).

%) and (34.52 %–89.02 % and 22.34 %–56.45 %) confirmed the anti-obesity and anti-diabetic activities of plants extract synthesized copper nanoparticles.

1. Introduction

Nanotechnology is a branch of science based on the synthesis, production, and use of materials [1]. Particles with a size ranging less than 100 nm are recognized as nanoparticles. It has become one of the most important emerging fields in science and technology with a wide range of applications such as agriculture, electronics, catalyst, bio-medical, sensors, optical fibers, bio-labeling, antimicrobials, cosmetics, paint, physicochemical areas, drug delivery, bioengineering, semiconductors, automobiles, packaging [2]. As the specific surface area of nanoparticles increases, their biological effectiveness also tends to increase due to the corresponding increase in surface energy [3]. Nanoparticle synthesis is based on various conventional methods. The two basic approaches of nanoparticle synthesis are the "Top-down" process (Mechanical, Chemical, Thermal, Laser, Explosion) and the "Bottom-down" process (Electrochemical/Chemical, Vapour deposition, Atom/Molecular, Laser, Spray, Sol-gel Process, Green Synthesis). In the top-to-bottom process, by size reduction appropriate bulk material breaks into fine size of particles, whereas the bottom-to-top process includes biological and chemical method synthesis of nanoparticles where self-assembly of atoms to nuclei takes place [4]. The synthesis of nanoparticles by conventional methods comprises some limitations bound to it as chemically synthesized nanoparticles exhibit the occurrence of some hazardous toxic compounds that are absorbed on the surface, which may later lead to some toxic effects on the medical field applications [5]. Various forms of metal nanoparticles have been used and comprise specific applications for particular metals such as gold nanoparticles (applications in fields such as tumor detection, specific delivery of drugs, genetic diseases and their diagnosis, photothermal therapy, angiogenesis, and photo imaging), silver nanoparticles (anti-cancer, antimicrobial, anti-inflammatory and for the treatment of various wounds), Iron nanoparticles (drug delivery, cancer therapy, cell labeling, tissue repair, immunoassays, hyperthermia, magnetic resonance imaging (MRI) and biological fluids detoxification), Titanium and Zinc nanoparticles (field of cosmetic, biomedical, (UV)-blocking agents and in different cutting edge processing), Palladium and Copper nanoparticles (optical limiting devices, batteries, plastics plasmonic waveguides, and polymers) [6,7]. Nanoparticles have also been used for the production of biosensors and electrochemical sensors, such as nanosensors used for the detection of mycobacteria, mercury content in drinking water, and algal toxins [8,9]. Nanoparticles synthesized through biosynthetic methods typically have well-defined morphology and size, in contrast to those produced by physicochemical methods. Furthermore, physicochemical methods can be expensive and may result in the production of hazardous and toxic chemicals. Copper nanoparticles possess unique properties that make them useful in various applications, including as antifungal, antibiotic, antimicrobial, and anti-fouling agents [10,11]. Copper nanoparticles (CuNPs) have been extensively researched for their antimicrobial properties against a variety of infectious microorganisms such as *Pseudomonas aeruginosa, Staphylococcus aureus, Bacillus subtilis, E.Coli, Syphillis typhus, Vibrio cholera, Klebsiella* [12–14]. A variety of methods have been employed for the synthesis of copper nanoparticles. These include electrochemical techniques, solid-state reactions, Sono chemical methods, microwave irradiation, alcohol thermal synthesis, quick precipitation, sol-gel methods, and liquid-liquid interface techniques. Each method offers unique advantages and challenges in terms of cost, scalability, control over particle size and morphology, and environmental impact [15,16]. For instance, the size and shape of nanoparticles can influence their physical and chemical properties, while the surface area can affect their reactivity. Dispersity refers to the distribution of sizes within a nanoparticle sample, which can impact the consistency of the sample's properties. The state of stability or aggregation can provide insights into how nanoparticles interact with each other and their environment. Lastly, the elemental composition can reveal the types of atoms present in the nanoparticles, which can be critical for certain applications [17]. Some of the basic techniques involved in the characterization of nanoparticles include Dynamic Light Scattering (DLS), UV–visible spectrophotometry, Fourier Transform Infrared Spectroscopy (FTIR), Powder X-Ray Diffraction (XRD), Transmission Electron Microscopy (TEM), Energy Dispersive Spectroscopy (EDS), and Scanning Electron Microscopy (SEM) [18].

Biological systems emerged as an alternative approach for the better synthesis of nanoparticles which are considered safe, eco-friendly, and have a special ability to produce nanoparticles of precise shape and controlled structures [19]. The use of naturally occurring reagents for the greener synthesis of nanoparticles majorly includes sugars, vitamins, biodegradable polymers, plant extracts, and microorganisms as a form of capping or reductant agents [20]. Synthesis of metal nanoparticles by biological method includes various parts of plants such as stem, root, leaf, latex, fruit, extracts, and seed [21]. The green synthesis process involves the use of various biomolecules found in plant extracts to reduce metal ions into nanoparticles [10]. Biomolecules such as proteins, organic acids, amino acids, vitamins, and various secondary metabolites like polyphenols, flavonoids, terpenoids, heterocyclic substances, polysaccharides, and alkaloids play a crucial role in the reduction of metal salts. These biomolecules also act as stabilizing and capping agents for the synthesized nanoparticles [22,23]. The demand for the development of new drugs whereas the primary focus occurs on bioactive compounds that are naturally endowed in plant sources and show higher medicinal and chemotherapeutic properties such as higher antioxidant properties due to flavonoids and phenols as a major constituent that help in the protection of cell damage from the free radicals, anti-inflammatory, anti-cancerous properties [24–26]. In this study, we report the green synthesis of copper nanoparticles (CuNPs) using plant extracts of *Bauhinia variegate* (KL) and *Saussure lappa* (SL) flower as reducing and stabilizing agents. We characterize the synthesized nanoparticles using various techniques such as UV–visible spectroscopy, FTIR, SEM, EDS, and PXRD. We also evaluate the antimicrobial, anti-obesity, and anti-diabetic activities of the plant-synthesized CuNPs. The novelty of the present study indicates that nanoparticles with a combination of herbal sources show potential inference for both health-related fields and the environment.

2. Material and methods

2.1. Material

Bauhinia variegate (KL) and *Saussure lappa* (SL) flowers were obtained from Himachal Pradesh as shown in Fig. 1. Analytical grade chemicals were used such as Potassium iodide, Sodium acetate, Sodium cholate, Copper sulphate, Acetic acid, Tri's base, lipase, Sodium hydroxide, Nitric acid, Iodine crystal, Lecithin, Glycerol trioleate, and Hydrochloric acid which were procured from Sigma Aldrich, St. Louis, MO, USA. Nutrient agar and Antibiotic (Ampicillin) were used of HiMedia, Mumbai, India. Bacterial cultures such as *Pseudomonas aeruginosa* (MTCC 424), *Escherichia coli* (MTCC 443), *Staphylococcus aureus* (MTCC 3160), and *Klebsiella pneumonia* (MTCC 3384) were procured from the Microbial Type Culture Collection (MTCC), Institute of Microbial Technology, Chandigarh, India. "A" certified glassware, Milli Q water, and double distilled water were used in the whole study.

2.2. Cleaning and drying

Bauhinia variegate (KL) and *Saussure lappa* (SL) flowers were cleaned with tap water thrice and once with triple distilled water to remove all the impurities. After that, both flower samples were dried through a tray dryer (PPI FiniX72) at a temperature of 40 °C for 42 h. Then the dried samples were ground with a grinder (MRC SM-450TR) to convert into a fine powder (Mesh sieve number 120 with 125 μm mesh aperture size) [6].

2.3. Extraction

Bauhinia variegate (KL) and *Saussure lappa* (SL) flower powder were mixed with water in a ratio (1:10) and the extraction was done with an orbital shaker (Orbitek LT-Orbital Laboratory Incubator Shaker) method at temperature 40 °C at 150 rpm for 42–72 h. The cooled mixture was filtered with Watt man No. 1. The filtered extract was dried through a hot air oven (LHAOF-224) at 40 °C for 3 days. Then dried extract was collected and stored in refrigeration condition 4 °C [27].

2.4. Synthesis of copper nanoparticles (CuNPs) by using plant extract

KL and SL flowers were used for the reduction of copper sulphate by the following method. 1.25 g of copper sulphate solution (0.05 M) was taken in 100 mL conical flask and heated at 80 °C on a Hot plate (Thermo Fisher Scientific, Mumbai, India). Then, the addition of 0.25 mL of plant extract dropwise with a micropipette during constant stirring on a magnetic stirrer (M3D, Eltak DIGIMAG, India). Blue to green colour was obtained, which confirmed the reduction in copper sulphate, and the reaction was completed. For optimization of plant stabilized CuNPs, the concentration of copper sulphate was kept constant (25 mL), and different concentrations of plant extract of KL and SL flower (1 %, 2 %, 3 %, 5 %, 6 %, 7 %, and 10 %) were used, respectively [28].

2.5. Characterization of copper nanoparticles

2.5.1. UV–visible spectrophotometer

UV–Visble Spectrophotometer (Evolution 201, Thermo Fischer Scientific India Pvt. Ltd, Mumbai) used to determine the concentration of the solution and presence of organic compounds in plant extract between 500 and 280 nm range [29].

2.5.2. Fourier Transform Infrared Spectroscopy (FTIR)

To determine the presence of different functional groups present in herbal extract FTIR (Agilent Technology) was used at a range

Fig. 1. *Bauhinia variegate* (KL) (left) and *Saussure lappa* (SL) flower (right).

650–4000 cm^{-1} with Attenuated Transmission (ATR) and an internal reflection accessory comprised of Composite Zinc Selenide (ZnSe) and Diamond 144 crystals (Shimadzu IR Prestige-21 equipment) [6].

2.5.3. Microstructure by scanning electron microscopy (SEM)

SEM (JEOLJSM-6510LV, INCA, USA) was used to determine the microstructure of plant-synthesized CuNPs at an acceleration voltage of 15 KV under high vacuum (9.0×10^{-5} torr) and micrographs were recorded [6].

2.5.4. Energy dispersive X-ray spectroscopy (EDS)

EDS was used for elemental analysis and chemical characterization of the samples. It is an analytical technique that relies on the interactions between electromagnetic radiation and matter. In EDS, the elemental analysis was performed using OXFORD EDS, which measured the intensity of the X-ray signals generated by the electron beam when it struck the surface of the sample [30].

2.5.5. X-ray diffraction (XRD)

X-ray Diffraction is a technique used to study the crystallographic structure, physical properties, and chemical composition of bulk, films, and nanomaterials. To determine crystal structure Bragg's law is used and XRD patterns revealed about the internal strain and crystalline size of plants stabilized CuNPs [31].

2.5.6. Dynamic light scattering (DLS)

Dynamic light scattering technique was used to determine the particle size of plant synthesized CuNPs, which is based on Mie-scattering theory with particle size analyzer (ZETA Sizers nanoseries (Malveen Instruments Nano ZS) [30].

2.6. Agar-well diffusion method

The Agar well diffusion method was used to evaluate the antibacterial activity of plant-synthesized CuNP extracts by measuring the inhibition zone diameter of wells. The plates were incubated at 37 °C for 24 h, and the growth inhibition of the test microorganisms was compared to a positive control using ampicillin [32].

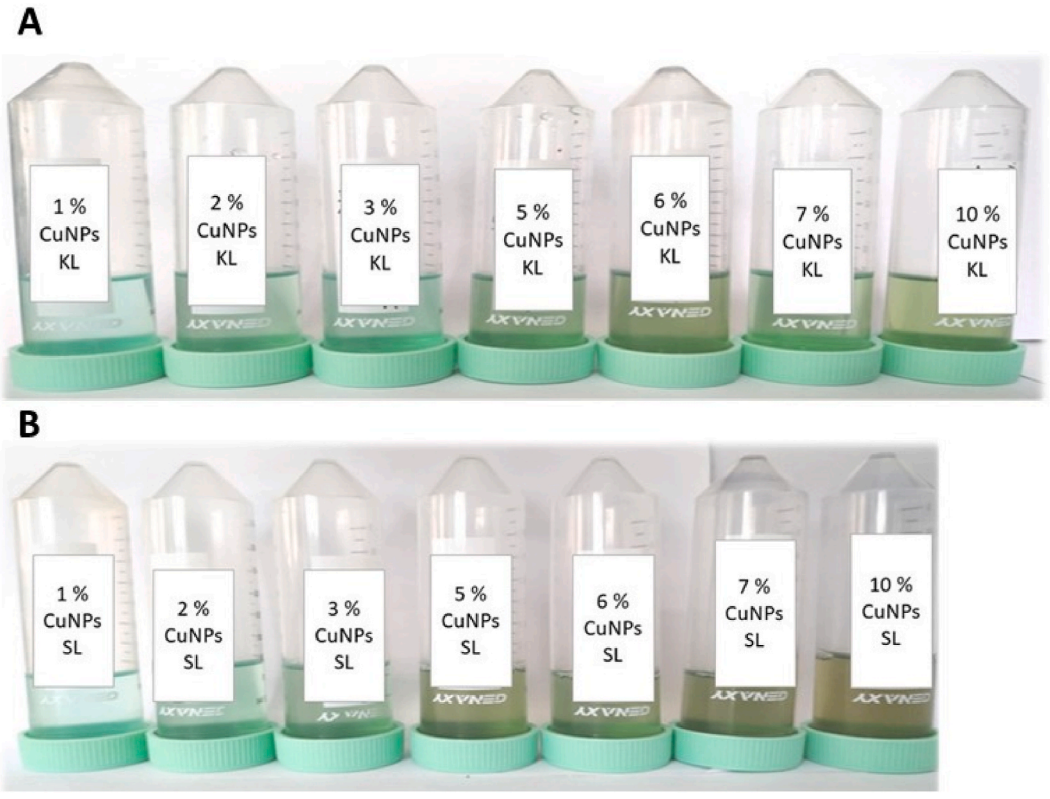

Fig. 2. Plant synthesized CuNPs at different concentration (Fig. 2.A. KL and Fig. 2.B. SL).

2.7. Lipase inhibition assay

The procedure of Kumar et al. [27], was used with minor modifications for the determination of lipase inhibitory assay of plant-synthesized CuNPs extracts. In 9 ml of 0.1 M TES buffer (pH 7.0), substrate solution was prepared by dissolving 10 mg lecithin, 5 mg sodium cholate, and 80 mg glycerol trioleate. 2 ml of sample and 2 ml of substrate solution with 1 ml of lipase was added and incubated at 37 °C for 30 min. The optical density was recorded at 550 nm using a UV spectrophotometer.

2.8. Amylase inhibition assay

As per the procedure of Kumar et al. [32], the estimation of amylase inhibition activity was determined using a UV–visible spectrophotometer (Evolution 201, Thermo Fischer Scientific India Pvt. Ltd, Mumbai) with minor modifications. For substrate solution, in 0.4 M NaOH (25 ml) 500 mg of soluble starch was mixed and heated for 5 min at 100 °C. pH of 7.0 was maintained by using HCl and then the 100 ml of volume was made using distilled water. Using acetate buffer (pH 6.5), different concentrations of plant extract solution were made. 200 μL of sample was mixed with 400 μL of substrate and 200 μL of α-amylase solution and incubated for 15 min at 25 °C. Thereafter, 800 μL of 0.1 HCl was added to terminate the reaction and then 2000 μL 1 mM iodine solution was added. At 650 nm, the optical density was measured using a UV–visible spectrophotometer.

2.9. Statistical analysis

As per the procedure of Kaushik et al., 2018 [29], standard error mean and one-way analysis of variance (statistical difference) were calculated through Microsoft Excel, 2019 (Microsoft Corp., Redmond, WA, USA).

3. Result and discussion

The present investigation focused on the synthesis and optimization of plants' synthesized CuNPs, as well as characterization and *in-vitro* analysis.

3.1. Synthesis and optimization of synthesized CuNPs

Reducing copper sulphate pentahydrate with plant extracts of KL and SL, which are responsible for the CuNPs green synthesis. The visual color change from blue to green indicates the formation of CuNPs Fig. 2 (A and B). The CuNPs were then stabilized with different concentrations of the plant extracts (1 %, 2 %, 3 %, 5 %, 6 %, 7 %, and 10 % for both plants). The optimal concentration of CuNPs was determined by UV–visible spectroscopy, as shown in Fig. 3 A, B, C, D. The UV–visible spectra showed a strong absorption peak between 500 and 280 nm for all the samples, which corresponds to the surface plasmon resonance (SPR) of CuNPs. The SPR peak did not shift with increasing plant extract concentration, suggesting that the shape and size of the CuNPs were not affected by the plant extracts. The

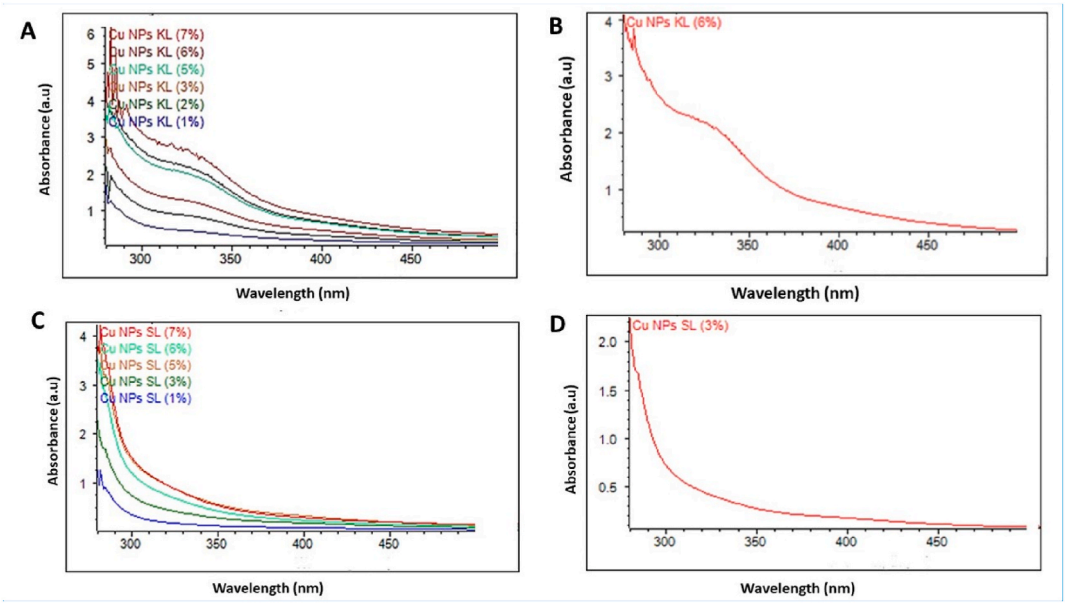

Fig. 3. UV–Visible Spectrum of different concentrations of plant Synthesized CuNPs (Fig. 3.A: Different Concentrations of KL Synthesized CuNPs, Fig. 3.B: 6 % selected KL based CuNPs Fig. 3.C: Different Concentrations of SL Synthesized CuNPs, and Fig. 3.D: 3 % selected SL based CuNPs).

selected concentrations for further characterization of the plant-synthesized CuNPs were 6 % for KL and 3 % for SL.

3.2. Characterization of plants synthesized CuNPs

3.2.1. Average particle size

Dynamic light scattering (DLS) analysis was used to check the average particle size of copper nanoparticles synthesized using plant extracts. The results, as shown in Fig. 4.A and 4.B revealed that the particle sizes for KL and SL were 8.721 nm and 98.03 nm, respectively. It showed that the correlation of nanoparticle concentration and the average particle size was increased. The UV–visible characterization showed lower absorbance values for both SL and KL, with particle sizes ranging between 1 and 100 nm. Consequently, these samples were selected for further characterization and application due to their optimal properties. This results in a larger average particle size due to the interaction and coalesce that occur between the free copper molecules during the minimum availability of binding sites in the plant extract. It has been reported that iron nanoparticles prepared with *Glycyrrhiza glabra* L leaf extract had 11–18 nm of particle size [33,33,34]. Similarly, 10–40 nm particle size was reported for AuNPs, which were synthesized by *Lens culinaris* seed aqueous extract [35]. Hashem et al., 2023 [36] reported that Tri-CSZ NPs were synthesized with *Aspergillus niger* which shows the average size of the particle (26.3 nm).

3.2.2. Fourier Transform Infrared Spectroscopy (FTIR)

Fig. 5.A and 5.B represent the functional group present in KL and SL Synthesized CuNPs through FTIR at 4000 to 500 cm^{-1}. Results clearly unveiled that C ≡ C at 2100 cm^{-1} confirmed the Alkyne stretching vibrations at the variable intensity in KL synthesized CuNPs. It also contains the vibrational band between ranges of 3200–3600 cm^{-1}resembles to the (O═H) hydroxyl group at 3203 cm^{-1} with a broad and strong intensity which presents the H-bonded and stretched vibration. Furthermore, the presence of (C ≡ C) confirmed the Alkyne i.e., 2108 cm^{-1} and 2100 cm^{-1} stretching vibrations at variable intensity. Similarly, SL synthesized CuNPs show the (O═H) with board and strong intensity at 3253 cm^{-1}. The vibrational band 1620-1680 cm^{-1} resembles of Alkene group (C═C) i.e., 1648 cm^{-1} with stretched vibrations at variable intensity. 2243 cm^{-1} and 2183 cm^{-1} peaks showed the H-bonded vibration and alkyne group (C ≡ C), which present between 2100 and 2260 cm^{-1}. The various peak's location in the spectrum indicates that for the CuNPs synthesis, the plant extract requirement was diverse because it prevents the agglomeration of the nanoparticles, which contributes to the secondary structures [37]. [38] reported the presence of hydroxyl group, alkyne, and alkene group in plants synthesized copper nanoparticles. Similarly, major copper elements with minor functional compounds were confirmed through elemental analysis and reported by Ref. [39]. [40] reported *Alhagi maurorum* extract with FeNPs showed the presence of triterpenes, phenolic, and flavonoids, which are commonly known as secondary metabolites. The different peaks are observed, such as 1197 cm^{-1} (-C-O- stretching), 1407 cm^{-1} (C═C stretching), 2927 cm^{-1} (C–H stretching), and 3417 cm^{-1} (O–H stretching). Therefore, Dehnoee et al. [41] reported a huge number of different organic functional groups at different bands such as 1500–1750 cm^{-1} (C═O and C═C bonds), 1056 cm^{-1} (C–O), 2928 cm^{-1} (C–H), and 3356 cm^{-1} (OH groups) are observed in *H. persicum* extract which conjugated with AgNPs. These bands prove the presence of phenolic and flavonoid compounds present in AgNPs with *H. persicum* extract. However, *Rhus coriaria* L. fruit aqueous extract used for synthesis of AuNPs l shows the presence of several antioxidant and secondary compounds at different peaks such as 1038 cm^{-1} (C–OH bands for proteins or polysaccharides), 1383 cm^{-1} (C═O for carboxylic acid group), 1623 cm^{-1} (C–O groups), 3287 cm^{-1} (OH groups of phenols and alcohols) respectively [42].

3.2.3. Microstructure and morphological characteristics of KL and SL synthesized copper CuNPs through scanning electron microscopy (SEM)

SEM was used to observe the morphology and structural characterization of plants synthesized CuNPs as depicted in Fig. 6. A Micrograph of plants synthesized CuNP powder showed the particles of different diameters, which are found to be poly-dispersed and

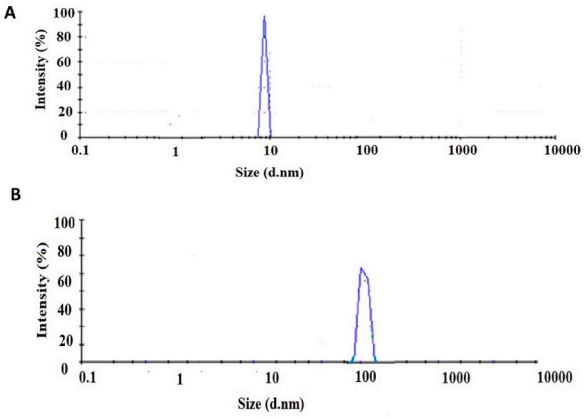

Fig. 4. A and 4.B average particle size of KL and SL synthesized CuNPs.

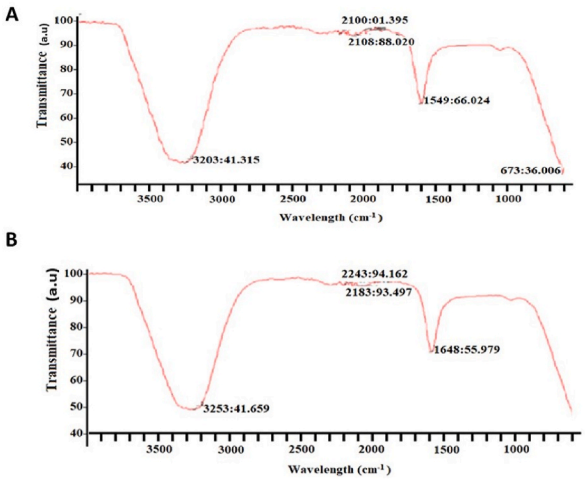

Fig. 5. A and 5.B FTIR Spectroscopy spectrum of KL and SL Synthesized CuNPs.

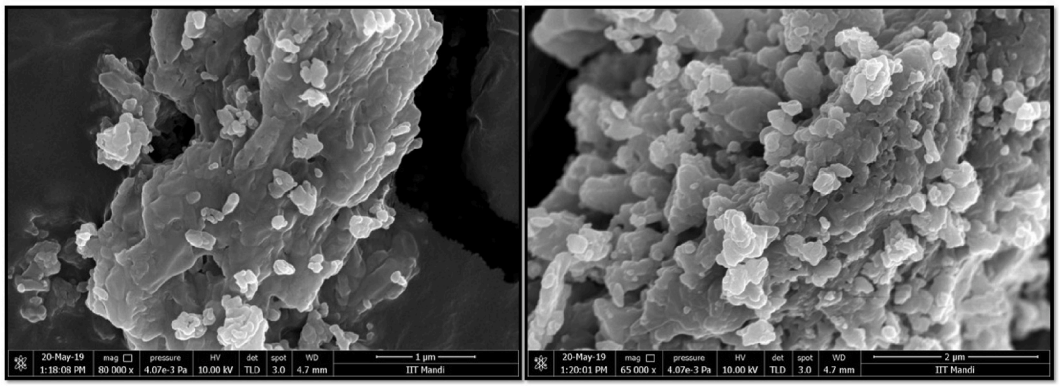

Fig. 6. Scanning Electron Microscopy (SEM) of KL (left) and SL synthesized CuNPs (right).

distributed. These plants' synthesized CuNPs appear to be predominantly in different shapes, irregular surfaces with small and different shape-like structures with irregular edges. This could be due to the synthesis of the copper nanoparticles with the plant extract. Dehnoee et al. [41] reported that the extract of H. persicum shows changes in metabolite arrangement and AgNPs adjustment. Similarly, *H. persicum* extract with AgNPs showed the homogeneous uniformity of silver, oxygen, nitrogen, and carbon elements through map screen images [42] reported the agglomeration structure for gold nanoparticles which are conjugated with *Rhus coriaria* L. fruit aqueous extract due to the presence of hydroxyl groups. However, agglomeration was also observed in Fe_3O_4 NPs with the synthesis of pectin molecules during manual preparation [43]. [40] reported a spherical shape for FeNPs, whereas plant extract helps in biosynthesized iron oxide and it works like a capping agent.

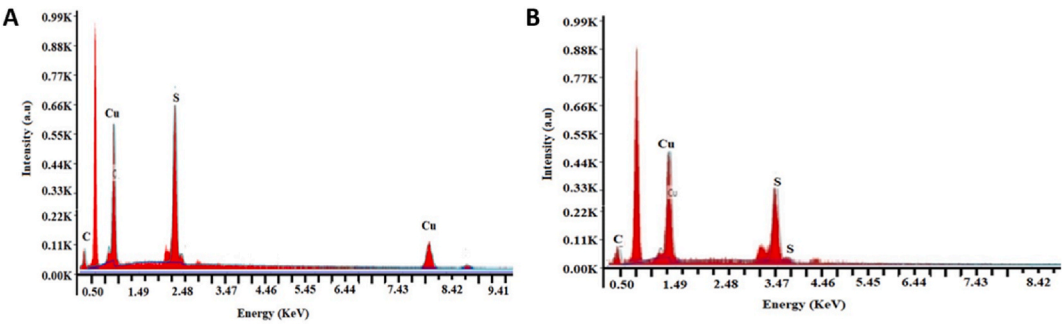

Fig. 7. A and 7.B EDS Spectrum of KL and SL synthesized CuNPs.

3.2.4. Energy dispersive X-ray spectroscopy (EDS)

EDS analysis can provide both qualitative and quantitative data of the elements that were used in the fabrication of nanoparticles as shown in Fig. 7.A and 7.B that represent the elemental composition of nanoparticles. At 1 KeV and 8 KeV and 9 KeV for KL and 0.95 KeV for SL showed the highly intense peak of elemental copper in the spectrum, which confirmed the stabilization of CuNPs with plant extracts. In addition, the presence of sulphur at 2.15 KeV, Carbon at 0.2 KeV, and Sulphur at 2.30 KeV for KL and Carbon at 0.2 KeV and Sulphur at 2.2 KeV and 2.4 KeV were also present all around the peak due to synthesis of plants extracts. In the synthesis of copper nanoparticles copper sulphate was used, which confirms the presence of sulphur. Thus, XRD confirms the presence of pure copper in plant-synthesized copper nanoparticles. Dehnoee et al., 2024 [44] reported *Thymus fedtschenkoi* leaf extract, which biosynthesized CuNPs, showed a weak peak (carbon, sulphur, and oxygen elements) and a strong peak such as copper element for elemental compounds. Similarly, it also revealed the development of biomolecules (originate the carbon and oxygen elements) which bind with CuNPs surface due to the presence of total phenolic compounds in the extract. Dehnoee et al. [41] reported the uniform peak of silver, nitrogen, oxygen, phosphorous, and carbon in AgNPs, which were surrounded with *Heracleum persicum* fruit extract. Similarly, it has been also reported that nanocomposite surfaces modified with pectin Fe_3O_4NPs showed a homogeneous dispersion of Au, Fe, and C atoms [43].

3.2.5. Powder X-ray diffraction (PXRD)

Internal strain and crystalline structure of different sizes of plants synthesized CuNPs were revealed through XRD patterns, as shown in Fig. 8.A and 8.B. It was observed that plants synthesized CuNPs are crystalline in nature and clearly showed a series of diffraction peaks. The diffraction peaks indicated the small crystal size and Scherrer formula, ($D = 0.9\ \lambda/\beta\ \mathrm{Cos}\ \theta$, where λ is the wavelength of X-ray radiation, β is the full width at half maximum (FWHM) of the peaks at the diffracting angle θ) were used to check the average crystallite size of plants synthesized CuNPs. A similar crystalloid structure and XRD spectrum have been supported by Ref. [45] for the *Gliricidia* leaf extract AgNPs which show the reduction of Ag^+ ions. Dehnoee et al., 2024 [44] reported that the CuNPs with *Thymus fedtschenkoi* leaf extract showed a highly crystalline nature at different sharp peaks 2θ are 43.24°, 50.39°, and 74.09°. These peaks clearly informed about the face-centered cubic structure of copper. However, FeNPs with plant extract showed crystallinity in structure with the peaks at different 2θ values such as 35.23°, 37.31°, 54.03°, 61.38°, and 75.37° [40]. Li et al., 2020 [43] reported the crystalline structure for the pectin-modified Fe_3O_4NPs, which show the cubic spinel peak at different degrees of 2θ (30.4°, 35.9°, 43.2°, 54.1°, 57.2°, and 63.1°).

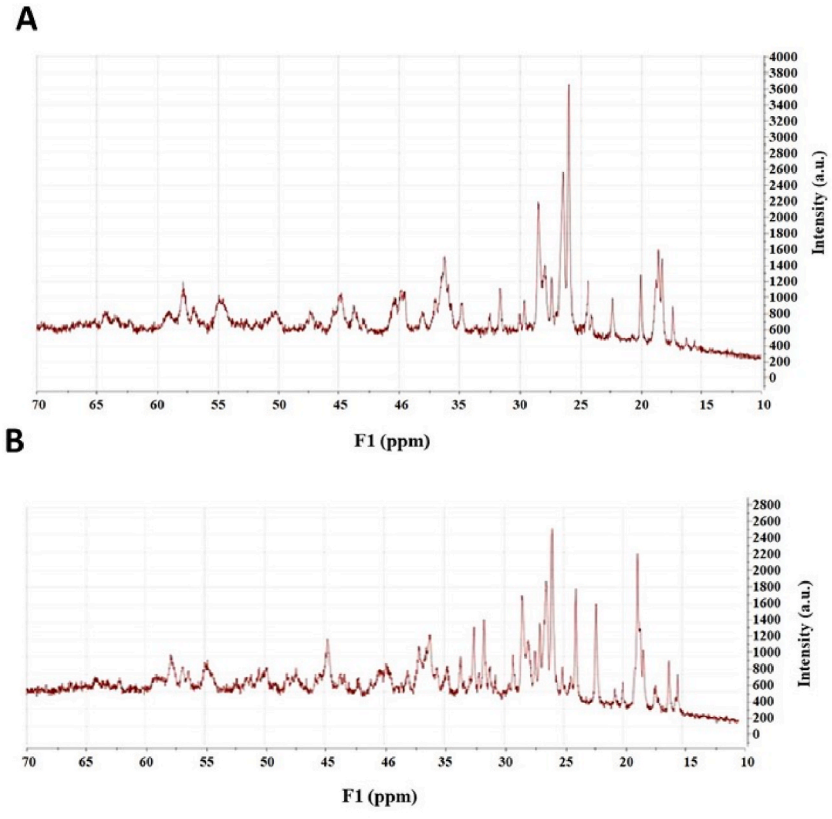

Fig. 8. A and 8.B PXRD of KL and SL synthesized CuNPs.

3.3. Antibacterial activity and antimicrobial activity

Fig. 9.A, B, C, and D represent the antibacterial activity of KL and SL Synthesized CuNPs against four bacterial cultures such as *Klebsiella pneumoniae*, *Escherichia coli*, *Staphylococcus aureus,* and *Pseudomonas aeruginosa* against the positive control i.e., antibiotic (Ampicillin) and the distilled water as the negative control. The zone of inhibition for KL (17 mm, 18 mm, 19 mm, and 18 mm) and SL (17 mm, 19 mm, 18 mm, and 18 mm) respectively for synthesized CuNPs against different strains as shown in Fig. 10.A and B. The present study shows a higher antibacterial activity due to different bacterial pathogens. Release of Cu^{+} ions and attachment to the bacteria cell walls in CuNPs which are also responsible for bactericidal activity [46] reported penetration also occurs inside the membrane surface due to the presence of metal ions [26] reported that CuNPs were surrounded with *Allium eriophyllum boiss* leaf aqueous extract and showed a significantly ($p < 0.05$) higher antibacterial activity as compared with all antibiotic standards. According to WHO, antimicrobial resistance is the microorganism's resistance to treat infections and works like an antimicrobial drug [47]. Whereas it reported that chitosan showed antimicrobial properties with amino group [48]. Hashem et al., 2023 [36] reported that Tri-CSZ NPs showed higher antifungal properties against all fungal strains such as *M. racemosus* (56 mm), *R. microspores* (43 mm), *L. corymbifera* (25 mm), and *S. racemosum* (52 mm). Similarly, it reported the MIC value of Tri-CSZ NPs for *M. racemosus* (1.95 μg/mL), *R. microspores* (7.81 μg/mL), *L. corymbifera* (62.5 μg/mL), and *S. racemosum* (3.9 μg/mL). Therefore, ZnO–CuO NPs showed significantly ($p < 0.05$) higher MIC value with *C. neoformans* (1000 μg/mL) as compared with *C. albicans* (500 μg/mL), *E. coli* and *S. aureus* (125 μg/mL), *B. subtilis* (31.25 μg/mL), and *A. brasiliensis* (15.62 μg/mL) [49]. [1] reported CuONPs showed significantly ($p < 0.05$) higher antimicrobial properties due to changes occurred in the transfer of macro and micro nutrients in cells through the destruction of barrier components inside the system.

3.4. Lipase inhibition assay

Fig. 11 represents the percentage of lipase inhibition assay with different concentrations and IC_{50} of plant-synthesized CuNPs. The study revealed that with an increase in concentration (20 μg/ml to 100 μg/ml) the percentage of lipase inhibition assay significantly ($p < 0.05$) increased in KL synthesized CuNPs (12.34 %–59.67 %) as compared with SL synthesized CuNPs (10.50 %–47.01 %). Similarly, the IC_{50} value for KL-synthesized CuNPs (64.21) is significantly ($p < 0.05$) higher as compared with SL-synthesized CuNPs (60.01). As compared with the literature, observed *Achillea millefoliumrubra* seeds showed the percentage of lipase inhibition and IC_{50} were 43.21 % and 24.67 [50]. [27] reported that *Saussurea lappa* root extract showed a percentage of lipase inhibition and IC_{50} (75.75 %, and 62.47). Similarly, it reported in Nigella sativa seeds plant-synthesized CuNPs with an increase in concentration from 20 μg mL to 1 to 80 μg mL−1, the percentage of lipase inhibition significantly ($p < 0.005$) increased from 33.20 % to 66.00 %, whereas the IC_{50} value is 57.54 [32]. The fat absorption in the body was reduced due to the presence of flavonoid content in Saussurea lappa [28,32]. *Bauhinia variegata* help in the hydrolysis process to convert dietary lipids into fatty acids. Therefore, it also observed that alkaloids and

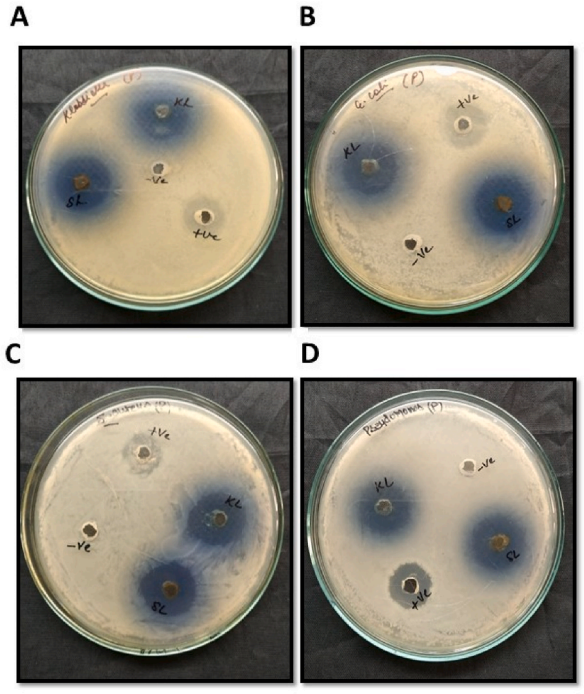

Fig. 9. Antibacterial Activity of KL and SL Synthesized CuNPs i.e., (Fig. 9.A) *Klebsiella pneumoniae* (Fig. 9.B) *Escherichia coli* (Fig. 9.C) *Staphylococcus aureus* (Fig. 9.D) *Pseudomonas aeruginosa.*

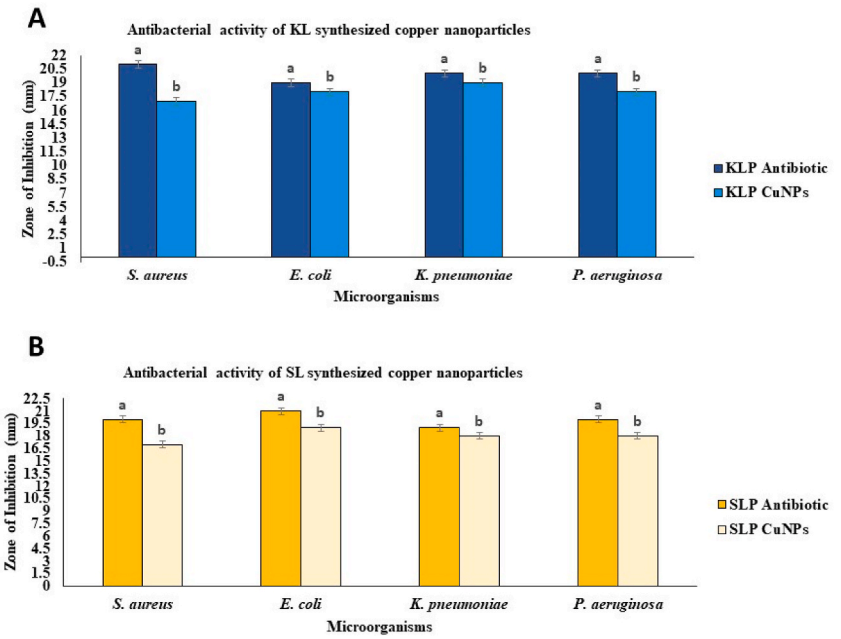

Fig. 10. A and 10.B Antimicrobial activity of KL and SL Synthesized CuNPs i.e., (a) *Staphylococcus aureus* (b) *Escherichia coli* (c) *Klebsiella pneumoniae* (d) *Pseudomonas aeruginosa*. Data are presented as mean ± SD ($n = 3$). [a-b] Means with the same superscript in a column do not vary significantly ($p < 0.05$) from each other.

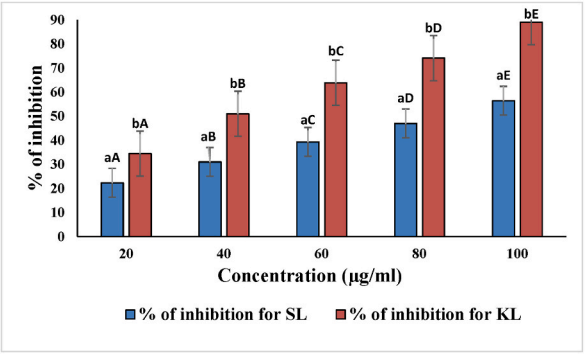

Fig. 11. Percentage of lipase inhibition assay (%) of SL and KL synthesized CuNPs.

flavonoids present in *Bauhinia variegate* help in reducing the breakdown of triglyceride [51]. A combination of herbs also helps in controlling the fat digestion process by removing the fat content from the body during the gastrointestinal process [27,32,50].

3.5. Amylase inhibition assay

The results of the Amylase Inhibition Assay are represented in Fig. 12. It shows an increase in concentration (20 µg/ml to 100 µg/ml), the percentage of amylase inhibition significantly ($p < 0.05$) increased in KL synthesized CuNPs (34.52 %–89.02 %) as compared with SL synthesized CuNPs (22.34 %–56.45 %) whereas, IC_{50} value 78.06 and 45.31. In a previous study by Ref. [27], it was reported that *Saussurea lappa* root extract showed a percentage of amylase inhibition and IC50 value of 75.41 % and 61.37, respectively. Similarly, it reported at 80 µg/mL concentration *Nigella sativa* seeds nanoparticles showed significantly ($p < 0.005$) higher inhibition effect and IC_{50} value (76.00 % and 46.34) [32]. Therefore, *Andrographis paniculata* shows a significantly ($p < 0.005$) lower amylase inhibition assay percentage and IC_{50} (3.29 % and 0.68). The specific mechanism shown by the *Saussurea lappa* and *Bauhinia variegate* helps in decreasing the content of carbohydrate digestion and glucose absorption by triggering the reduction in postprandial hyperglycemia. They also help reduce complex carbohydrate molecules through the enzymatic hydrolysis process [27,32].

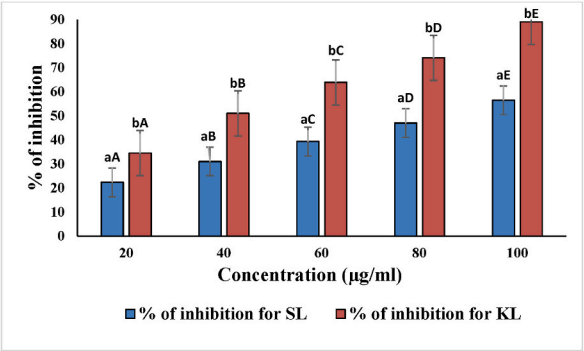

Fig. 12. Percentage of amylase Inhibition Assay (%) SL and KL Synthesized CuNPs.

4. Conclusions

Over many decades, plants have been used more due to higher therapeutic effects due to the presence of a huge number of bioactive compounds such as phenols, alkaloids, terpenoids, flavonoids, and many others. The bioactive compounds present in plants interact in the human body with biological systems, which show several effective properties such as anti-inflammatory, antioxidant, analgesic, antimicrobial, anxiolytic, antidepressant, immunomodulatory, cardioprotective, and hepatoprotective. Different experiment involves various methods for the isolation, extraction, and to check the efficacy of bioactive compounds present in plant sources. In conclusion, the present investigation demonstrated that the green synthesis of CuNPs using plant extracts is a feasible, eco-friendly, non-toxic, and economical method. The plant-synthesized CuNPs (SL and KL of concentration 3 % and 6 %, respectively), have promising applications in the fields of antibacterial, anti-obesity, and anti-diabetic. KL and SL showed average particle sizes of 8.721 nm and 98.03 nm. Whereas, KL synthesized CuNPs (IC_{50} 64.21 and IC_{50} 78.06) showed higher lipase and amylase inhibition assay as compared with SL synthesized CuNPs (IC_{50} 60.01 and IC_{50} 45.31). However, more research is needed to scale up the production of copper nanoparticles and to evaluate their toxicity, biocompatibility, and mechanism of action. CuNPs could be potentially used as food additives or nutraceuticals in the future.

Funding

The authors would like to extend their sincere appreciation to the Researchers Supporting Project Number (RSP2024R356), King Saud University, Riyadh, Saudi Arabia.

CRediT authorship contribution statement

Mukul Kumar: Writing – review & editing, Writing – original draft, Visualization, Validation, Supervision, Software, Resources, Methodology, Data curation, Conceptualization. **Deepika Kaushik:** Writing – original draft, Software, Resources, Methodology, Formal analysis, Data curation. **Ashwani Kumar:** Conceptualization. **Hari Krishnan:** Resources. **Fatih Oz:** Writing – review & editing, Supervision. **Charalampos Proestos:** Writing – review & editing, Resources. **Abeer Hashem:** Funding acquisition. **Elsayed Fathi Abd_Allah:** Funding acquisition.

Declaration of competing interest

The authors declare that they have no known competing financial interests or personal relationships that could have appeared to influence the work reported in this paper.

Acknowledgement

The authors would like to extend their sincere appreciation to the Researchers Supporting Project Number (RSP2024R356), King Saud University, Riyadh, Saudi Arabia.

References

[1] M.S. Hasanin, S. M, A.M. Youssef, Ecofriendly bioactive film doped CuO nanoparticles based biopolymers and reinforced by enzymatically modified nanocellulose fibers for active packaging applications, Food Packag. Shelf Life 34 (2022) 100979.

[2] A. Anisha, D. Kaushik, M. Kumar, A. Kumar, T. Esatbeyoglu, C. Proestos, M.R. Khan, T. Elobei, J. Kaur, F. Oz, Volarization of Brewer's spent grain for noodles preparation and its potential assessment against obesity, Int. J. Food Sci. Technol. 58 (6) (2023) 3154–3179. https://doi.org/10.1111/ijfs.16443.

[3] B. Hu, R. Liu, Q. Liu, Y. Shi, J. Li, L. Wang, L. Li, X. Xiao, Y. Wu, Engineering surface patterns on nanoparticles: new insights into nano-bio interactions, J. Mater. Chem. B 10 (14) (2022), https://doi.org/10.1039/D1TB02549J, 2357-238.

[4] S. Ahmed, M. Ahmad, B.L. Swami, S. Ikram, A review on plants extract mediated synthesis of silver nanoparticles for antimicrobial applications: a green expertise, J. Adv. Res. 7 (1) (2016) 17–28, https://doi.org/10.1016/j.jare.2015.02.007.

[5] A. Istiqola, A. Syafiuddin, A review of silver nanoparticles in food packaging technologies: regulation, methods, properties, migration, and future challenges, J. Chin. Chem. 67 (11) (2020) 1942–1956, https://doi.org/10.1002/jccs.202000179. Soc.

[6] M. Kumar, D. Kaushik, J. Kaur, C. Proestos, F. Oz, A. Kumar, A. Anjali, T. Elobeid, M.E. Terzioğlu, J. Xiao, Assessment of anti-obesity potential and techno-functional properties of bougainvillea spectabilis willd, Bracts. Separations 9 (12) (2022) 399, https://doi.org/10.3390/separations9120399.

[7] H. Ahari, L.K. Lahijani, Migration of silver and copper nanoparticles from food coating, Coat 11 (4) (2021) 380, https://doi.org/10.3390/coatings11040380.

[8] M.S. Sumitha, T.S. Xavier, Recent advances in electrochemical biosensors –A brief review, Hybrid Adv. (2023) 100023, https://doi.org/10.1016/j.hybadv.2023.100023.

[9] M. Zahran, Carbohydrate polymer-supported metal and metal oxide nanoparticles for constructing electrochemical sensors, Mater. Adv 5 (1) (2024) 68–82, https://doi.org/10.1039/D3MA00706E.

[10] S. Maqsood, S. Qadir, A. Hussain, A. Asghar, R. Saleem, S. Zaheer, N. Nayyar, Antifungal properties of copper nanoparticles against Aspergillus Niger, Sch. Int. J. Biochem. 3 (2020) 87–91, https://doi.org/10.36348/sijb.2020.v03i04.002.

[11] A. Saravanan, P.S. Kumar, S. Karishma, D.V.N. Vo, S. Jeevanantham, P.R. Yaashikaa, C.S. George, A review on biosynthesis of metal nanoparticles and its environmental applications, Chemosphere 264 (2021) 128580, https://doi.org/10.1016/j.chemosphere.2020.128580.

[12] A. Mishra, N. Mishra, N., Antiquorum sensing activity of Copper nanoparticle in pseudomonas aeruginosa: an in silico approach, Proc. Natl. Acad. Sci. India B Biol. Sci. 91 (2021) 29–36, https://doi.org/10.1007/s40011-020-01193-z.

[13] A. Tahir, C. Quispe, J. Herrera-Bravo, H. Iqbal, F. Anum, Z. Javed, A. Sehar, J. Sharifi-Rad, Green synthesis, characterization and antibacterial, antifungal, larvicidal and anti-termite activities of copper nanoparticles derived from Grewia asiatica L, Bull. Natl. Res. Cent. 46 (1) (2022) 1–11, https://doi.org/10.1186/s42269-022-00877-y.

[14] M.H. Ahmed, M.T. Javed, S.U.K. Bahadur, A. Tariq, M.H. Tahir, M.E. Tariq, N. Tariq, S. Zarnab, M.H. Ali, Antibacterial effects of copper oxide nanoparticles against E. coli induced infection in broilers, Appl. Nanosci. 12 (7) (2022) 2031–2044, https://doi.org/10.1007/s13204-022-02482-x.

[15] M.C. Crisan, M. Teodora, M. Lucian, Copper nanoparticles: synthesis and characterization, physiology, toxicity and antimicrobial applications, Appl. Sci. 12 (1) (2021) 141, https://doi.org/10.3390/app12010141.

[16] R. Lu, W. Hao, L. Kong, K. Zhao, H. Bai, Z. Liu, A simple method for the synthesis of copper nanoparticles from metastable intermediates, RSC Adv. 13 (21) (2023) 14361–14369, https://doi.org/10.1039/D3RA01082A, 2023.

[17] S. Dawadi, S. Katuwal, A. Gupta, U. Lamichhane, R. Thapa, S. Jaisi, G. Lamichhane, D.P. Bhattarai, N. Parajuli, Current research on silver nanoparticles: synthesis, characterization, and applications, J. Nanomater. (2021, (2021) 1–23, https://doi.org/10.1155/2021/6687290.

[18] S. Mourdikoudis, R.M. Pallares, N.T. Thanh, Characterization techniques for nanoparticles: comparison and complementarity upon studying nanoparticle properties, Nanoscale 10 (27) (2018) 12871–12934, https://doi.org/10.1039/C8NR02278J.

[19] L. Devi, P. Kushwaha, T.M. Ansari, A. Kumar, A. Rao, Recent trends in biologically synthesized metal nanoparticles and their biomedical applications: a review, Biol. Trace Elem. Res. 1–17 (2023), https://doi.org/10.1007/s12011-023-03920-9.

[20] M.K. Priya, P.R. Iyer, Biosynthesis and optimization of highly stable gold nanoparticles, nanoconjugates, nanodrug conjugates and chitosan nanoconjugates using medicinal plants, Bull. Natl. Res. Cent. 46 (1) (2022) 134, https://doi.org/10.1186/s42269-022-00824-x.

[21] I. Ahmed, F.A. Mir, J.A. Banday, Synthesis of metal and metal oxide nanoparticles using plant extracts—characterization and applications, BioNanoScience 13 (4) (2023) 1541–1557, https://doi.org/10.1007/s12668-023-01194-y.

[22] R. Álvarez-Chimal, J.A. Arenas-Alatorre, Green Synthesis of Nanoparticles. A Biological Approach, 2023, https://doi.org/10.5772/intechopen.1002203.

[23] S. Jadoun, R. Arif, N.K. Jangid, R.K. Meena, Green synthesis of nanoparticles using plant extracts: a review, Environ. Chem. Lett. 19 (2021) 355–374, https://doi.org/10.1007/s10311-020-01074-x.

[24] M. Ishaq, P. Taslimi, Z. Shafiq, S. Khan, R.E. Salmas, M.M. Zangeneh, A. Saeed, A. Zangeneh, N. Sadeghian, A. Asari, H. Mohamad, Synthesis, bioactivity and binding energy calculations of novel 3-ethoxysalicylaldehyde based thiosemicarbazone derivatives, Biol. Chem. 100 (2020) 103924, https://doi.org/10.1016/j.bioorg.2020.103924.

[25] A. Ahmeda, A. Zangeneh, M.M. Zangeneh, Green synthesis and chemical characterization of gold nanoparticle synthesized using Camellia sinensis leaf aqueous extract for the treatment of acute myeloid leukemia in comparison to daunorubicin in a leukemic mouse model. App, Org. Chem. 34 (3) (2020) e5290, https://doi.org/10.1002/aoc.5290.

[26] H. Zhao, H. Su, A. Ahmeda, Y. Sun, Z. Li, M.M. Zangeneh, M. Nowrozi, A. Zangeneh, R. Moradi, Biosynthesis of copper nanoparticles using Allium eriophyllum Boiss leaf aqueous extract; characterization and analysis of their antimicrobial and cutaneous wound-healing potentials, Appl. Organomet. Chem. 36 (12) (2022) e5587, https://doi.org/10.1002/aoc.5587.

[27] M. Kumar, S. Guleria, P. Chawla, A. Khan, V.K. Modi, N. Kumar, R. Kaushik, Anti-obesity efficacy of the selected high altitude Himalayan herbs: in vitro studies, J. Food Sci. Technol. 57 (2020) 3081–3090.

[28] P. Singh, Y.J. Kim, D. Zhang, D.C. Yang, Biological synthesis of nanoparticles from plants and microorganisms, Trends Biotechnol. 34 (7) (2016) 588–599, https://doi.org/10.1016/j.tibtech.2016.02.006.

[29] R. Kaushik, P. Chawla, N. Kumar, S. Janghu, A. Lohan, Effect of premilling treatments on wheat gluten extraction and noodle quality, Food Sci. Technol. Int. 24 (7) (2018) 627–636, https://doi.org/10.1177/1082013218782368, 2018.

[30] P. Jaglan, D. Kaushik, M. Kumar, A. Kumar, J. Kaur, E. Oz, C. Brennan, C. Proestos, M. Brennan, N. Ahmad, T. Elobeid, Structural, thermal, techno-functional and chemical characterization using fourier transform infrared spectroscopy, gas-chromatography-mass spectrophotometry, thermogravimetric analyser, field emission scanning electron microscopy and energy-dispersive x-ray spectrometer of moringa oleifera flower powder, Int. J. Food Sci. Technol. 58 (11) (2023) 5992–6005, https://doi.org/10.1111/ijfs.16707, 2023.

[31] A. Gargi, J. Singh, P. Rasane, S. Kaur, J. Kaur, M. Kumar, D. Sowdhanya, M. Gunjal, R. Choudhary, S. Ercisli, Effect of drying methods on the nutritional and phytochemical properties of pumpkin flower (Cucurbita maxima) and its characterization, J. Food Meas. Char. 17 (5) (2023) 5330–5343, https://doi.org/10.1007/s11694-023-02026-z.

[32] M. Kumar, D. Kaushik, A. Kumar, P. Gupta, C. Proestos, E. Oz, E. Orhan, J. Kaur, M.R. Khan, T. Elobeid, M. Bordiga, Green synthesis of copper nanoparticles from Nigella sativa seed extract and evaluation of their antibacterial and antiobesity activity, Int. J. Food Sci. Technol. (2023), https://doi.org/10.1111/ijfs.16359.

[33] N. Sebeia, M. Jabli, A. Ghith, T.A. Saleh, Eco-friendly synthesis of Cynomorium coccineum extract for controlled production of copper nanoparticles for sorption of methylene blue dye, Arab. J. Chem. 13 (2) (2020) 4263–4274, https://doi.org/10.1016/j.arabjc.2019.07.007.

[34] L. Ma, A. Ahmeda, K. Wang, A.R. Jalalvand, K. Sadrjavadi, M. Nowrozi, A. Zangeneh, M.M. Zangeneh, X. Wang, Introducing a novel chemotherapeutic drug formulated by iron nanoparticles for the clinical trial studies, App. Organ. Chem. 36 (12) (2022) e5498, https://doi.org/10.1002/aoc.5498.

[35] A. Ahmeda, M.M. Zangeneh, A. Zangeneh, Green formulation and chemical characterization of Lens culinaris seed aqueous extract conjugated gold nanoparticles for the treatment of acute myeloid leukemia in comparison to mitoxantrone in a leukemic mouse model, Appl. Organomet. Chem. 34 (3) (2020) e5369, https://doi.org/10.1002/aoc.5369.

[36] A.H. Hashem, A.A. Al-Askar, J. Haponiuk, K.A. Abd-Elsalam, M.S. Hasanin, Biosynthesis, characterization, and antifungal activity of novel trimetallic copper oxide–selenium–zinc oxide nanoparticles against some mucorales fungi, Micro 11 (6) (2023) 1380.

[37] M. Kumar, D. Kaushik, A. Kumar, P. Gupta, C. Proestos, E. Oz, E. Orhan, J. Kaur, M.R. Khan, T. Elobeid, M. Bordiga, Green synthesis of copper nanoparticles from Nigella sativa seed extract and evaluation of their antibacterial and antiobesity activity, Int. J. Food Sci. Technol. 58 (6) (2023) 2883–2892.

[38] Z.B. Shifrina, V.G. Matveeva, L.M. Bronstein, Role of polymer structures in catalysis by transition metal and metal oxide nanoparticle composites, Chem 120 (2) (2019) 1350–1396, https://doi.org/10.1021/acs.chemrev.9b00137. Rev.

[39] K.M. Rajesh, B. Ajitha, Y.A.K. Reddy, Y. Suneetha, P.S. Reddy, Assisted green synthesis of copper nanoparticles using Syzygium aromaticum bud extract: physical, optical and antimicrobial properties, Optik 154 (2018) 593–600, https://doi.org/10.1016/j.ijleo.2017.10.074.

[40] J. Bai, X. Gongsun, L. Xue, M.M. Zangeneh, Introducing a modern chemotherapeutic drug formulated by iron nanoparticles for the treatment of human lung cancer, J. Exp. Nanosci. 16 (1) (2021) 397–409, https://doi.org/10.1080/17458080.2021.1998460.
[41] A. Dehnoee, R. Javad Kalbasi, M.M. Zangeneh, M.R. Delnavazi, A. Zangeneh, One-step synthesis of silver nanostructures using Heracleum persicum fruit extract, their cytotoxic activity, anti-cancer and anti-oxidant activities, Micro & Nano Lett. 18 (1) (2023) e12153, https://doi.org/10.1049/mna2.12153.
[42] J. Liu, A. Zangeneh, M.M. Zangeneh, B. Guo, Antioxidant, cytotoxicity, anti-human esophageal squamous cell carcinoma, anti-human Caucasian esophageal carcinoma, anti-adenocarcinoma of the gastroesophageal junction, and anti-distal esophageal adenocarcinoma properties of gold nanoparticles green synthesized by Rhus coriaria L. fruit aqueous extract, J. Exp. Nanosci. 15 (1) (2020) 202–216, https://doi.org/10.1080/17458080.2020.1766675.
[43] Y. Li, N. Li, W. Jiang, G. Ma, M.M. Zangeneh, M. M, In situ decorated Au NPs on pectin-modified Fe3O4 NPs as a novel magnetic nanocomposite (Fe3O4/Pectin/Au) for catalytic reduction of nitroarenes and investigation of its anti-human lung cancer activities, Int. J. Biol. Macromol. 163 (2020) 2162–2171, https://doi.org/10.1016/j.ijbiomac.2020.09.102.
[44] A. Dehnoee, R. Javad Kalbasi, M.M. Zangeneh, M.R. Delnavazi, A. Zangeneh, A. Characterization, Anti-lung cancer activity, and cytotoxicity of bio-synthesized copper nanoparticles by Thymus fedtschenkoi leaf extract, J. Clu. Sci.e 35 (2024) 863–874, https://doi.org/10.1007/s10876-023-02512-w.
[45] Z. Huang, F. Cui, H. Kang, J. Chen, X. Zhang, C. Xia, Highly dispersed silica-supported copper nanoparticles prepared by precipitation− gel method: a simple but efficient and stable catalyst for glycerol hydrogenolysis, Chem. Mater. 20 (15) (2008) 5090–5099, https://doi.org/10.1021/cm8006233.
[46] T. Kruk, K. Szczepanowicz, J. Stefańska, R.P. Socha, P. Warszyński, Synthesis and antimicrobial activity of monodisperse copper nanoparticles, Colloids Surf., B 128 (2015) 17–22, https://doi.org/10.1016/j.colsurfb.2015.02.009.
[47] F. Prestinaci, P. Pezzotti, A. Pantosti, Antimicrobial resistance: a global multifaceted phenomenon, Pathog. Glob. Health 109 (7) (2015) 309–318.
[48] M. Saied, M. Hasanin, T.M. Abdelghany, B.H. Amin, A.H. Hashem, Anticandidal activity of nanocomposite based on nanochitosan, nanostarch and mycosynthesized copper oxide nanoparticles against multidrug-resistant Candida, Int. J. Biol. Macromol. 242 (2023) 124709.
[49] M.S. Hasanin, A.H. Hashem, A.A. Al-Askar, J. Haponiuk, E. Saied, A novel nanocomposite based on mycosynthesized bimetallic zinc-copperoxide nanoparticles, nanocellulose and chitosan: characterization, antimicrobial and photocatalytic activities, Electron. J. Biotechnol. 65 (2023) 45–55.
[50] N.M.P. Maideen, Prophetic medicine-Nigella Sativa (Black cumin seeds)–potential herb for COVID-19? JoP 23 (2) (2020) 62, https://doi.org/10.3831/KPI.2020.23.010.
[51] M. Patil, T. Anand, N. Ilaiyaraja, F. Khanum, F., In-vitro antioxidant and anti-obesity properties of Bauhinia Variegata, Defence Life Sci 2 (2017) 128–132, https://doi.org/10.14429/dlsj.2.11355. J.